GNSS/IRS hybridization : fault detection and isolation of more than one range failure

Anne-Christine Escher, Christophe Macabiau, Nicolas Martin, Benoit Roturier, Vincent Vogel

GNSS/IRS Hybridization: Fault Detection and Isolation of More than One Range Failure

Anne-Christine ESCHER, *ENAC*
Christophe MACABIAU, *ENAC*
Nicolas MARTIN, *THALES-AVIONICS*
Benoit ROTURIER, STNA
Vincent VOGEL, *ENAC*

BIOGRAPHY

Anne-Christine Escher graduated as an electronics engineer in 1999 from ENAC (Ecole Nationale de l'Aviation Civile) in Toulouse, France. Since 1999, she has been working on the application of satellite navigation techniques to civil aviation at the signal processing lab of the ENAC as a PhD. student.

Christophe Macabiau graduated as an electronics engineer in 1992 from ENAC (Ecole Nationale de l'Aviation Civile) in Toulouse, France. Since 1994, he has been working on the application of satellite navigation techniques to civil aviation. He received his Ph.D. in 1997 and has been in charge of the signal processing lab of the ENAC since 2000.

Nicolas Martin is graduated as an aeronautical engineer in 1994 from ENSAE (Ecole nationale Supérieure de l'Aéronautique et de l'Espace) in Toulouse, France. Since 1995 he has been working for THALES Avionics (in Valence) in inertial navigation, INS/GNSS hybridization and integrity fields. He is currently working on Galileo signal and receiver definition.

Benoit Roturier graduated as a CNS systems engineer from Ecole Nationale de l'Aviation Civile (ENAC), Toulouse in 1985 and obtained a PhD in Electronics from Institut National Polytechnique de Toulouse in 1995. He was successively in charge of Instrument Landing Systems at DGAC/STNA (Service Technique de la Navigation Aerienne), then of research activities on CNS systems at ENAC. He is now head of GNSS Navigation subdivision at STNA and is involved in the development of civil aviation applications based on GPS/ABAS, EGNOS and Galileo.

Vincent Vogel graduated in June 2002 as an electronics engineer from the ENAC.

ABSTRACT

GPS/IRS hybridization is a good candidate to fulfill demanding civil aviation requirements. When the integrity of the GPS measurements is ensured they may be used to calibrate inertial position and improve accuracy. This can be done in a tightly coupled manner by means of a Kalman filter. Calibrated IRS can ensure coasting while maintaining good short term accuracy and helps detect large GPS failures.

The hybridized system must also be able to detect slowly growing errors on GPS measurements that may affect inertial calibration. These errors may affect one or several GPS measurements.

Fault detection and exclusion capacity of Receiver Autonomous Integrity Monitoring is limited for GPS, as it is designed for one satellite failure only. Therefore other solutions have been proposed. Among these are the extrapolation method and the solution separation method that are also designed to detect one satellite failure at a time.

The study reported in this paper presents first results obtained with an extension of Mats Brenner's separation algorithm for fault detection. That extension concerns detection and isolation of more than one failure during operations ranging from en-route to NPA, with the objective of satisfying the availability requirement.

The paper starts with a brief review of the classical Solution Separation method for a single satellite failure detection and isolation. In this section the model of the tightly coupled GPS/IRS system involved in simulations is also presented. The third section is dedicated to theoretical description of the one failure Solution separation fault detection and exclusion algorithm.

The next section considers the behavior of the algorithm when two simultaneous range failures occur. In particular the impact of two faulty measurements on the test metrics in the former fault detection and exclusion algorithm is examined. These simulation results are used to discuss the contribution of a two range failure detection algorithm.

Afterwards, a two simultaneous range failure detection and exclusion algorithm based on an extension of the nominal Solution Separation method is introduced. Definitions of performance parameters (Horizontal Protection Level, Horizontal Exclusion Level, and Missed Detection Probability), when several pseudo range failures (ramp, bias, etc.) occur simultaneously, are discussed. Finally initial simulation results are presented.

I. INTRODUCTION

In GPS/IRS hybridization, GPS measurements are used as observations of the integration processor which provides estimates of inertial errors. These estimates are on one hand added to IRS output to form the navigation solution to the pilot (position, velocity, Euler angles). They are on the other hand used to calibrate the inertial platform (nominal position, velocity and Euler angles, and inertial error sources compensation). Thus when GPS data are unavailable, the calibrated IRS can ensure the navigation continuity.

However, several types of perturbations can affect the signal processed by a GPS receiver and thus lead to a corrupted inertial calibration. Since inertial navigation systems greatly depend on initial conditions, this may have a great incidence on solution navigation accuracy.

GPS perturbations are thermal noise, atmospheric disturbances, multipath and interference. Interference remains the most feared perturbation for civil aviation users because it can affect several tracking channels at a time during a long period.

Efficient failure detection and isolation algorithms have been designed ensuring high availability and integrity monitoring of GNSS navigation means, but they have been implemented assuming that there is a unique satellite failure.

For this reason, there is a need to appreciate the ability of fault detection and exclusion algorithms to detect and isolate multiple range failures.

As a first step the following paper discusses the use of Solution Separation theory to achieve two-failure detection and isolation.

II. SOLUTION SEPARATION METHOD

Fault detection and exclusion function of the Solution Separation algorithm consists in maintaining a primary Kalman filter which incorporates the N measurements of the whole system, as many Kalman sub-filters as the number of tracked satellites (i.e. N sub-filters), and for each of these sub-filters a bank of N-1 sub-sub-filters using measurements of N-2 satellites.

Initially, the primary filter F_{00} provides an estimate of IRS error in order to form the inertial corrected position at the output of the whole system.

Sub-filters which each of these incorporate the measurements from N-1 satellites are dedicated to detection only. They are noted F_{0n} , $n = 1 \ldots N$.

Sub-sub-filters are dedicated to exclusion. Each of these is excluding the measurement excluded by its "parent" sub-filter, and the measurement from a different satellite. They are noted F_{nm} with $n = 1 \ldots N, m = 1 \ldots N$ and $n \neq m$.

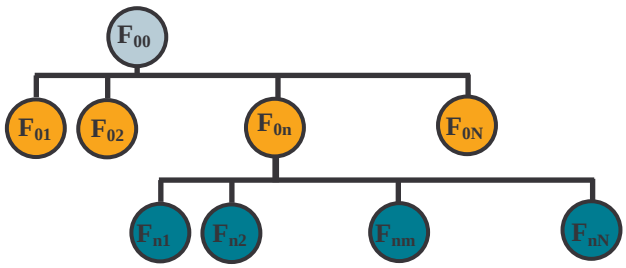

Figure 1. Detection and exclusion filters hierarchy

Fault detection

Solution separation between F_{00} and each F_{0n} is estimated: it is the difference in the horizontal/vertical plane between the state vector estimated by F_{00} and the state vector estimated by F_{0n} .

Fault detection is performed by monitoring the separation between the main-solution and each of sub-solutions and comparing it to a computed detection threshold that depends on the separation statistics and the false detection probability P_{FD} which is deduced from false alarm rate. When a failure occurs at least one solution separation will exceed this threshold. This method also guarantees a protection radius against any failure (even slow ramp) in straight relationship with the threshold and the value of the required missed detection probability P_{MD} .

Fault exclusion

Fault exclusion assumes that there is only one satellite failure at a time.

When there is a detection, the separation between each sub-sub-filter and its parent sub-filter is computed and compared to an exclusion threshold that depends on the expected separation statistics and P_{FD} . If for sub-filter F_{0n} , there exists one solution separation such that one separation between it and sub-sub-filter F_{nm} exceeds the threshold, it can't be the faulty satellite. But if there is only one sub-filter F_{0n} for which all separations between its solution and its sub-sub-filters F_{nm} are under the threshold, satellite n is the faulty satellite.

After exclusion succeeds, the sub-filter which has not used measurement from the failed satellite becomes the primary filter. Its sub-sub-filters are the new bank of detection filters.

All of the Kalman filters are running in the same way.

II. GPS/IRS KALMAN HYBRIDIZING FILTERS

All measurements and simulations have been made with Matlab.

This section presents the models we have implemented.

For any of the Kalman filters, the implemented system is composed of three units: an inertial unit – Inertial

Reference System - (Inertial measurement Unit + Strapdown calculator), a GNSS receiver (GPS measurements) and an integration process (Kalman filters) that also performed FDE function. Figure 2.

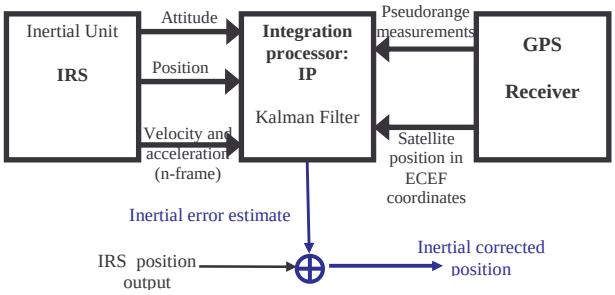

Figure 2. GPS/IRS architecture

Inertial unit

It provides to the integration process Matlab-generated inertial position, velocity and attitude angles and gyrometric and accelerometric measurements.

The Inertial Measurement Unit generates realistic gyro and accelero measurements at $100\ Hz$ rate from trajectory definition and attitude angles evolution of an aircraft.
Sensor noises and biases have also been modelled.

IMU measurements are processed by Strapdown inertial navigation to provide inertial solution at $100\ Hz$: mobile positions and velocities relative to the earth frame in the navigation frame, and the attitude angles of the mobile body frame to the navigation frame.

GPS Receiver

Pseudo range measurements (PRs) are generated at $1Hz$. Random noise is added on each satellite range measurement and is composed of a white-Gaussian noise due to noise process (b_{PR}).

GPS/IRS Kalman filtering

As shown in figure 2, the position output by the whole system is the corrected inertial position. The role of Kalman filters is to estimate inertial errors using GPS measurements in order to correct inertial outputs.

Kalman filtering state model

The dynamical evolution of the system is given by inertial error model equations. The measurement vector consists of the difference between two PRs to each satellite (GPS PR and predicted PR computed with inertial data).
Each component δx of the Kalman filter state vector stands for the difference between the true value x and the measured $\tilde{x}$ (or computed $\hat{x}$) value.
The state vector is a 17 error state variable

$$\Delta\mathbf{X} = [\boldsymbol{\rho}, \boldsymbol{\delta v}, \boldsymbol{\delta p}, \boldsymbol{\delta\omega}, \boldsymbol{\delta f}, \boldsymbol{\delta b}]^T$$

where

- $\boldsymbol{\rho}$ Attitude error vector- 3 states
- $\boldsymbol{\delta v}$ Inertial velocity error vector- 3 states
- $\boldsymbol{\delta r}$ Inertial position error:
  - δL latitude error
  - δG longitude error
  - δh altitude error
- $\boldsymbol{\delta\omega}$ Gyro drift – 3 states
- $\boldsymbol{\delta f}$ Accelero bias – 3 states
- $\boldsymbol{\delta b}$ Receiver clock error vector- 2 states

Many different inertial error models are available in literature. They are actually equivalent [5]. In our system the inertial navigation error model applied is

$$\begin{aligned}
\dot{\boldsymbol{\rho}} &= \boldsymbol{\delta\omega} + \boldsymbol{\omega}^{n}_{In} \times \boldsymbol{\rho} \\
\dot{\boldsymbol{\delta v}} &= \boldsymbol{\delta f} + \left(\boldsymbol{\omega}^{n}_{Ie} + \boldsymbol{\omega}^{n}_{In}\right) \times \boldsymbol{\delta v} + \boldsymbol{\rho} \times \mathbf{a}^{n}_{mI} \\
\dot{\boldsymbol{\delta r}} &= \boldsymbol{\delta v} + \boldsymbol{\omega}^{n}_{en} \times \boldsymbol{\delta r}
\end{aligned} \qquad (1)$$

where

- $\mathbf{a}^{m}_{mI}$ accelerometric measurement: inertial non-gravitational acceleration of the mobile in the mobile frame
- $\boldsymbol{\omega}^{n}_{In}$ rotation rate of the navigation frame relative to the inertial frame in the navigation frame
- $\boldsymbol{\omega}^{n}_{Ie}$ Earth rotation rate in the navigation frame
- $\boldsymbol{\omega}^{n}_{en}$ rotation rate of the navigation frame relative to the Earth frame in the navigation frame

Using inertial data as nominal trajectory these non-linear equation are linearized and lead to the matrix presentation of the dynamical evolution equation of the linearized Kalman filter [6]:

$$\dot{\mathbf{X}} = \mathbf{F} \cdot \mathbf{X} + \mathbf{v} \qquad (2)$$

where

- $\mathbf{F}$ is the state transition matrix
- v is the state noise vector. It is a zero-mean Gaussian white noise vector, whose components are all independent

Let Φ be the discrete form of $\mathbf{F}$.
Let Q be the state noise covariance matrix:

$$\mathbf{Q} = E\left[\mathbf{v} \cdot \mathbf{v}^T\right] \qquad (3)$$

Kalman filtering measurement model

Each component of the measurement vector $\mathbf{z}$ at filter input is the difference between two PRs to each satellite. One is the measured PR input from the GPS receiver; the other is the predicted PR computed on the basis of the satellite positions obtained from the GPS receiver and the user location as calculated by the IRS.

The coefficients of the measurement matrix $\mathbf{H}$ are direction cosines computed from the GPS navigation equation linearization.
Let $\mathbf{R}$ be the measurement noise covariance matrix: all measurement noises are independent.

The size of the $\mathbf{z}-$vector and of the $\mathbf{R}$ and $\mathbf{H}-$matrices depends on the number of tracked satellite.

Kalman filters implementation

Let ij be the subscript for the Kalman filter F_{ij}. The maximum number of tracked satellites is $N = 10$.
There is one primary filter, N sub-filters, and N*(N-1) sub-sub-filters that are running in parallel.
The estimated state vector for each are

primary filter: $\boldsymbol{\Delta}\hat{\mathbf{x}}_{\mathbf{00}}$

sub-filter: $\boldsymbol{\Delta}\hat{\mathbf{x}}_{\mathbf{0n}}$, $n = 1, N$

sub-sub-filter: $\boldsymbol{\Delta}\hat{\mathbf{x}}_{\mathbf{nm}}$, $n = 1, n; m = 1, N; m \neq n$

The estimation error covariance matrix for each is

primary filter: $\mathbf{P}_{\mathbf{00}}$

sub-filter: $\mathbf{P}_{\mathbf{0n}}$, $n = 1, N$

sub-sub-filter: $\mathbf{P}_{\mathbf{nm}}$, $n = 1, n; m = 1, N; m \neq n$

where

$$\mathbf{P}_{\mathbf{ij}} = E\left[\boldsymbol{\delta}\mathbf{x}_{\mathbf{ij}} \cdot \boldsymbol{\delta}\mathbf{x}_{\mathbf{ij}}{}^{T}\right],\ \boldsymbol{\delta}\mathbf{x}_{\mathbf{ij}} = \boldsymbol{\Delta}\hat{\mathbf{x}}_{\mathbf{ij}} - \boldsymbol{\Delta}\mathbf{x}$$

Δx is the true error between estimated IRS and true position: $\Delta x = \hat{X}_{IRS} - X$

Because GPS and IRS data are not available at the same rate, the error model is updated at $100Hz$ and Kalman filters measurements are updated at $1Hz$.
So the Kalman corrections are available every second.

Next section details implementation of FDE algorithm using Kalman filters parameters.

III. FAULT DETECTION AND EXCLUSION FUNCTION WITH KALMAN FILTERS

Fault detection function

At each estimation time the discriminator for the n[th] sub-filter is based on Solution Separation vector between the primary filter and the n[th] sub-filter:

$$\begin{aligned}\mathbf{dx}_{\mathbf{0n}}{}^{+}(k) &= \boldsymbol{\Delta}\hat{\mathbf{x}}_{\mathbf{00}}{}^{+}(k) - \boldsymbol{\Delta}\hat{\mathbf{x}}_{\mathbf{0n}}{}^{+}(k) \\ &= \boldsymbol{\delta}\mathbf{x}_{\mathbf{00}}{}^{+}(k) - \boldsymbol{\delta}\mathbf{x}_{\mathbf{0n}}{}^{+}(k),\ n = 1 \ldots N\end{aligned} \tag{4}$$

whose statistics are described by the covariance matrix

$$\mathbf{dP}_{\mathbf{0n}}{}^{+}(k) = E\left[\left(\mathbf{dx}_{\mathbf{0n}}{}^{+}(k)\right) \cdot \left(\mathbf{dx}_{\mathbf{0n}}{}^{+}(k)\right)^{T}\right] \tag{5}$$

with $^{+}(k)$ stands for a posteriori state vector estimate at time k.

The statistic of the horizontal separation vector $\mathbf{X}_{\mathbf{H}} = \mathbf{dx}_{\mathbf{0n}}{}^{+}[7:8]$, is described by $\mathbf{L}_{\mathbf{0n}} = \mathbf{dP}_{\mathbf{0n}}{}^{+}[7:8,7:8]$.
Because separations on North and East axes are correlated, $\mathbf{L}_{\mathbf{0n}}$ is projected in an orthogonal plane so that,

$$\mathbf{L}_{\mathbf{0n}} = \mathbf{P}_{\perp} \cdot \boldsymbol{\Delta} \cdot \mathbf{P}_{\perp}{}^{\mathbf{T}} \tag{6}$$

and $\mathbf{X}_{\perp} = \mathbf{P}_{\perp}{}^{T} \cdot \mathbf{X}_{\mathbf{H}}$ is a Gaussian vector whose covariance matrix is the diagonal matrix $\boldsymbol{\Delta}$ (eigenvalues matrix of $\mathbf{L}_{\mathbf{0n}}$).
One of the two eigenvalues is dominating. Let λ^{dP} be the variance ($\boldsymbol{\Delta}(1,1)\ or\ \boldsymbol{\Delta}(2,2)$) of the dominating error in the horizontal plane.

For each sub-filter the decision threshold - D_{0n} - is set so that the test metric d_{0n} will exceed D_{0n} with the probability P_{FD}. Since all sub-filters have the same chance of false alarm

$$D_{0n} = \sqrt{\lambda^{dP}} \cdot Q^{-1}\left(\frac{P_{FD}}{2N}\right) \tag{7}$$

with

$Q^{-1}(u) = erfc(u)$

P_{FD} is the false detection probability [see Table1].

and $d_{0n} = \left|X_{\perp}(1)\right|\ or\ \left|X_{\perp}(2)\right|$ (8)

depending on $\lambda^{dP} = \boldsymbol{\Delta}(1,1)\ or\ \lambda^{dP} = \boldsymbol{\Delta}(2,2)$.
Indeed $\mathbf{L}_{\mathbf{0n}}$ is degenerated, the test metrics norm value is only expressed in $\left|X_{\perp}(1)\right|$ or $\left|X_{\perp}(2)\right|$.

The test for detecting one satellite failure is

- H_0 no detection: $d_{0n} < D_{0n}$
- H_1 detection: $\exists n \in \{1, N\}, d_{0n} \geq D_{0n}$

[test 1]

Horizontal protection level HPL

By definition *HPL* is the error bound that contains the primary filter error with a probability of $1 - p_{MD}$ when $d_{0n} = D_{0n}$ [2].

Since for each sub-filter

$$\boldsymbol{\delta x}_{\mathbf{00}}^{+}(k) = \mathbf{dx}_{\mathbf{0n}}^{+}(k) + \boldsymbol{\delta x}_{\mathbf{0n}}^{+}(k),\ n = 1 \ldots N \quad (9)$$

at detection (for the n[th] subset)

$$HPL_n = D_{0n} + a_{0n} \quad (10)$$

where a_{0n} is an upper bound of the n[th] sub-filter horizontal error $\Delta\mathbf{x}_{\mathbf{0n}}^{+}[7:8]$ whose distribution is described by $\mathbf{L} = \mathbf{P}_{\mathbf{0n}}^{+}[7:8,7:8]$.

Let $\lambda^{P_{0n}}$ be the maximum eigenvalue of $\mathbf{L}$

$$a_{0n} = \sqrt{\lambda^{P_{0n}}} \cdot Q^{-1}(1 - p_{MD}) \quad (11)$$

Besides we have to consider the rare normal performance that is to say the contribution of the primary filter HPL_0

$$HPL_0 = \sqrt{\lambda^{P_{00}}} \cdot Q^{-1}\left(\frac{P_{ff}}{2}\right) \quad (12)$$

where P_{ff} is the rare normal performance rate and $\lambda^{P_{00}}$ the maximum eigenvalue of $\mathbf{P}_{\mathbf{00}}^{+}[7:8,7:8]$.

The horizontal protection level is

$$HPL = \max\{HPL_0, \max(HPL_n)\}, n = 1, N \quad (13)$$

Fault exclusion function

Fault exclusion is accomplished in the same manner than detection but one layer down in the filters hierarchy.

The discriminator of each of the sub-sub-filter is the separation between each sub-sub-filter estimate solution and its parent's sub-filter estimate solution in the horizontal plane. For the n[th] sub-filter they are

$$\begin{aligned}\mathbf{dx}_{\mathbf{nm}}^{+}(k) &= \Delta\hat{\mathbf{x}}_{\mathbf{0n}}^{+}(k) - \Delta\hat{\mathbf{x}}_{\mathbf{nm}}^{+}(k) \\ &= \boldsymbol{\delta x}_{\mathbf{0n}}^{+}(k) - \boldsymbol{\delta x}_{\mathbf{nm}}^{+}(k),\ \ m = 1 \ldots N, m \neq n\end{aligned} \quad (14)$$

whose statistics are described by the covariance matrix $\mathbf{dP}_{\mathbf{nm}}^{+}(k)$.

Since the N sub-systems formed by the N sub-filters are tested in an independent manner, for each sub-sub-filter the decision threshold is set so that (assuming that each filter F_{nm} has the same chance for a false alarm)

$$D_{nm} = \sqrt{\lambda^{dP_{nm}}} \cdot Q^{-1}\left(\frac{P_{FD}}{2(N-1)}\right) \quad (15)$$

The test statistic associated to D_{nm} is

$$d_{nm} = |X_{m\perp}(1)| \ or \ |X_{m\perp}(2)| \quad (16)$$

Satellite r is excluded as the failed satellite if and only if [test 2]

$d_{rm} < D_{rm}$ for all $m \neq r$

and

$d_{nr} \geq D_{nr}$ for all $r \neq n$

Horizontal exclusion level HEL

HEL is the error bound that contains the primary filter error with a probability of $1 - p_{FE}$ when the failure is excluded.

"For a failed exclusion to occur, the solution of one of the sub-filters $\Delta\hat{\mathbf{x}}_{\mathbf{0n}}$ which does contain the failed satellite must be separated from one of its sub-sub-filter's solution $\Delta\hat{\mathbf{x}}_{\mathbf{nm}}$ by less than the threshold D_{nm} plus the sub-sub-filter position error" [2]

Let a_{nm} be the sub-sub-filter horizontal estimation error bound and $\lambda^{P_{nm}}$ be the maximum eigenvalue of $\mathbf{P}_{nm}^{+}[\mathbf{7:8,7:8}]$: $a_{nm} = \sqrt{\lambda^{P_{nm}}} \cdot Q^{-1}(1 - p_{FE})$.

For the nth sub-filter HEL_n is given by

$$HEL_n = \max\{D_{nm} + a_{nm}\}, m = 1, N \quad (17)$$

The horizontal exclusion level is

$$HEL = \max\{HEL_n\}, n = 1, N \quad (18)$$

as defined in [9]

IV. TWO-FAILURE DETECTION AND EXCLUSION WITH A ONE-FAILURE ASSUMPTION FDE ALGORITHM – SIMULATION RESULTS

Failures impact on test metrics of row 2

Let b be the pseudo range bias vector when measurements on channel i and j are affected by bias of value b_i and bias b_j respectively

$$b = \begin{bmatrix} 0 & \cdots & 0 & \underset{i}{b_i} & 0 & \cdots & 0 & \underset{j}{b_j} & 0 & \cdots & 0 \end{bmatrix}^T,$$

Since $\mathbf{dx}_{mn}$ and $\boldsymbol{\delta x}_{\mathbf{0}m}$ are statically dependent, let us form the 34x1 error vector

$$\boldsymbol{\delta x}^{+}(k) = \left[\boldsymbol{\delta x}_{\mathbf{0}m}^{+}(k), \Delta\mathbf{x}_{mn}^{+}(k)\right]^T$$

whose statistics are described by $\mathbf{dP}_{\mathbf{0n}}^{\mathbf{dual}+}(k)$

One can show that the impact of b (at its first time of apparition) on the test metrics which links sub-filter F_{0m} to sub-sub-filter F_{mn}, with $m = 1 \ldots N, m \neq n$, is

$$\delta x^{+}(k) = \Sigma(k) \cdot \delta x^{-}(k) + \Gamma(k) \cdot w_{0m}(k) + \Gamma(k) \cdot b(k)$$

with

$$\Sigma = \begin{bmatrix} I - \mathbf{K}_{0m} \cdot \mathbf{H}_{0m} & 0 \\ (\mathbf{K}'_{mn} - \mathbf{K}_{0m}) \cdot \mathbf{H}_{0m} & I - \mathbf{K}'_{mn} \cdot \mathbf{H}_{0m} \end{bmatrix}$$

$$\Gamma = \begin{bmatrix} \mathbf{K}_{0m} \\ \mathbf{K}_{0m} - \mathbf{K}'_{mn} \end{bmatrix}$$

$\mathbf{K}_{mn}$ is the Kalman gain of filter F_{mn}.

$\mathbf{K}'_{mn}$ is constructed from $\mathbf{K}_{mn}$ so that it operates on the full set of measurements by extending the 17x(N-1) matrix $\mathbf{K}_{mn}$ sub-solution matrix with a nth zeroed column.

Since $E\left[\delta x^{+}(k) \cdot (\delta x^{+}(k))^{T}\right] = P_{mn}^{dual}(k)$,

with, $P_{mn}^{dual}(k) = \Sigma(k) \cdot (P_{mn}^{dual}(k))^{-} \cdot (\Sigma(k))^{T} + \Gamma(k) \cdot R_{0m}(k) \cdot (\Gamma(k))^{T}$, when the two simultaneous range failures assumption is made we may theoretically expect that there is no sub-filter F_{0m} for which there is no test metrics d_{mn} which won't exceed its threshold.
In other words we may expect that there is no sub-filter F_{0m} for which two simultaneous range failures have no impact at row 2 of Kalman filters.
For the following we denote this state as "simultaneous impact" [figure 3].

Let assume that SAT1 and SAT2 are at channels 2 and 4

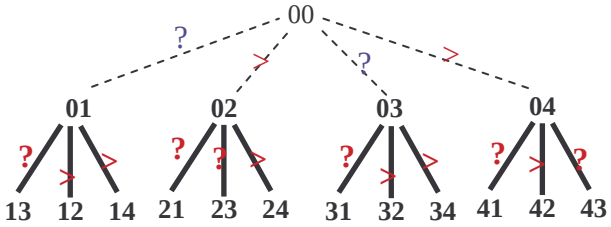

Figure 3. Test metrics vs decision threshold: simultaneous impact.

Yet simulations we have conducted have put the stress on the "transition states" which may exist.
A reason for this is that under no-failure condition, all test metrics involved at rows 1 and 2 in the Kalman filters hierarchy are lower than their respective decision threshold [see figure 4]. The presence of the two failures implied these test metrics to become progressively larger than their decision thresholds and this even for the sub-filters which exclude one of the two failures.

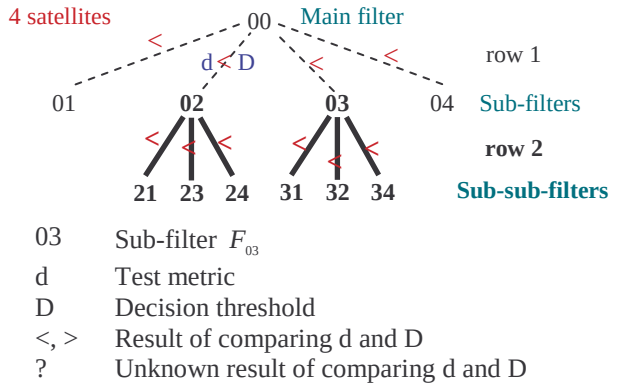

Figure 4. Test metrics vs decision threshold: no-failure case.

Depending on the constellation and the range failures size value, due to noise process in GPS measurements, the impact of one of the two failures may be delayed such as there is one of the sub-filters for which tests metric at row 2 are all inferior to their decision threshold.
In that case if condition of [test 2] is fulfilled, the satellite tested by this sub-filter may be excluded from the constellation [see figure 5].
It is similar to two successive one range failure assumptions.
For the following we denote this phenomenon as "delayed impact".

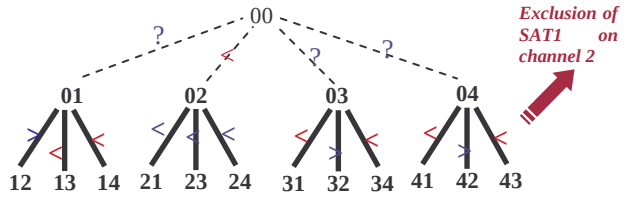

Figure 5. Test metrics vs decision threshold: delayed impact.

Yet, there is a risk to exclude a wrong satellite, but we may assume it is greatly reduced since in [test 2] we identify the faulty satellite for each of the subset which contains a detection alarm.

Simulations background

Failures setting

Two ramp failures are added to the measurements of the worst two case satellites; that is to say the pair of tracking satellites for which the two ramps will produce the greatest SLOPE: SLOPEmaxmax. The calculation of SLOPEmaxmax is performed according [7].
Let SAT1 and SAT2 be the faulty satellites.

Civil aviation requirements

Appendix R to RTCA/DO 229C [3] clarifies FDE requirements to GPS/IRS application for en-route to non-precision approach. (Table 1)

Missed detection probability	0.001
False detection rate (SA off)	1/3 10^{-6}/hr
Probability (p_{MI}) of exceeding HPL	10^{-7}/hr
Rare normal performance rate	$<10^{-7}$/sample
Failed exclusion probability	0.001
Continuity	1/3 10^{-6}/hr

Table 1. FDE requirements.

These requirements are defined assuming that there is only one satellite failure at a time.

Simulation conditions

- GPS constellation: mask angle 5° (no change)
- GPS receiver: total measurement noise 12.5m (1σ)
- Inertial error sources

These errors are added on accelero and gyro measurements at the IMU output

Gyrometer constant bias	0.01 °/hr
Gyrometer white noise	3.10^{-5} °/s/$\sqrt{Hz}$
Accelerometer constant bias	50 µg
Accelerometer white noise	6.4 µg/$\sqrt{Hz}$

Table 2. Good IRS error sources

- GPS/IRS hybridization is performed in an open-loop manner.

FDE algorithm

- No. of independent tests/hr=4
- $P_{FA} = 1/3.10^{-6}\ /\ hr = 1/12.10^{-6}\ /\ test$
- $P_{ff} = 1/3.10^{-8}\ /\ test$
- ramp errors (m/s) are added simultaneously at time t_0 on satellites SAT1 and SAT2.

We are interesting in the Horizontal error.

Simulations results

Delayed failure impacts

In the case in which failures impact is delayed, failures behave such as there were two successive failures. The classical Solution Separation FDE algorithm is able to detect and isolate them.

To illustrate this, the following simulation was performed:

- Table 3: simulation hypothesis
- Figure 6 and Table 4: simulation results on position error

Number of tracked satellites = 9, t_0 = 300s		
SAT1	channel: 3	error size: 1m/s
SAT2	channel: 9	error size: 0.7m/s

Table 3: Simulation hypothesis: delayed failure impacts

	delay after t_0	
	detection	isolation
SAT1	47 s	51 s
SAT2	69 s	74 s

Table 4: Time of detection and isolation

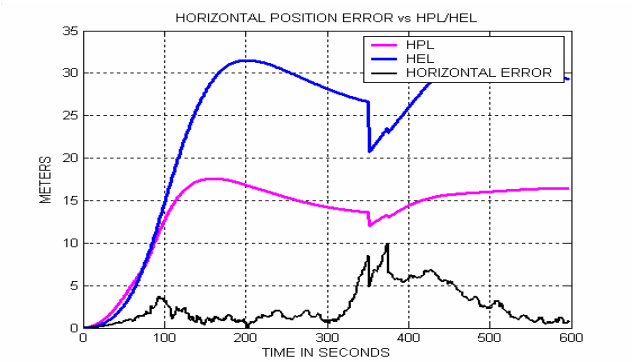

Figure 6: Horizontal position error vs HPL/HEL

Despite the success of isolating the two faulty satellites, the impact of the faulty measurements is not negligible on the horizontal position solution.

After isolation of SAT1, the error size is of 5 m and is getting growing due to a miss-initialization of Kalman filters. Indeed, F_{00} is initialized with F_{0SAT1} which is still running with SAT2 faulty measurements. This corrupted initialization is creating an additional error on position solution; this error is growing to 10m until isolation of SAT2.

At time 373, the horizontal error size is reduced to 6.5m.

Despite no Monte-Carlo simulations have been conducted, simulations have shown that the error size after isolation greatly depends on the constellation. In fact long-duration simulations – with fixed-positioning trajectory assumptions – have shown that the delay after isolation for Kalman filter re-convergence depends on constellation.

Simultaneous failure impacts

In the more rare case in which failures impact is simultaneous, the classical Solution Separation FDE algorithm is no more able to isolate them. The first row of Kalman filters is effectively detecting failures, but the test at the second row can't find any sub-filter for which all the tests metric between it and its parents sub-sub-filters are under their decision threshold.

This is a failed exclusion case that leads to a true alert [8].

To illustrate this, the following simulation was performed:

- Table 5: simulation hypothesis
- Figure 7 and Table 6: simulation results on position error

Number of tracked satellites = 9, t_0 = 300s		
SAT1	channel: 3	error size: 0.7m/s
SAT2	channel: 9	error size: 1m/s

Table 5: Simulation hypothesis: simultaneous failure impacts

Delay after t0	detection: 60s	isolation: none

Table 6: Time of detection

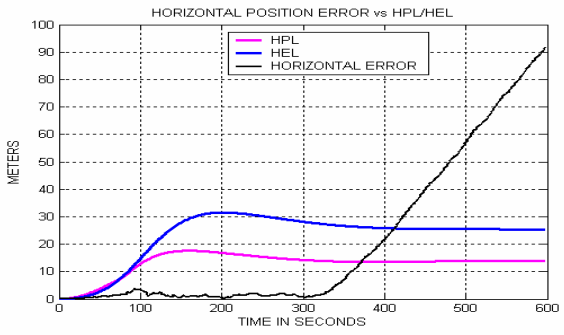

Figure 7: Horizontal position error vs HPL/HEL

This impossibility to isolate the two failures may be solved by adding one more Kalman filters layer: sub-sub-sub-filters which each one is excluding measurements from 3 satellites of the constellation [see figure 8]

V. PRINCIPLE OF ISOLATING TWO FAILURES

Principle

Isolation of two failures is performed by estimating the solution separations between sub-sub-filters and sub-sub-sub-filters - $\mathbf{dx}_{mnp}$, forming test metrics - d_{mnp}, and comparing them with their correspondent decision threshold - D_{mnp}.

In the nominal case, the entire tests results are negative. When there are two failures, there is no sub-filter for which all the tests metric between it and its parents' sub-sub-filters are under their decision threshold. But, there exists only two sub-sub-filters F_{nm} and F_{mn} for which all separations between their solution and their sub-sub-sub-filters solution are under the corresponding thresholds. Thus satellites n and m are claimed as the faulty satellites.

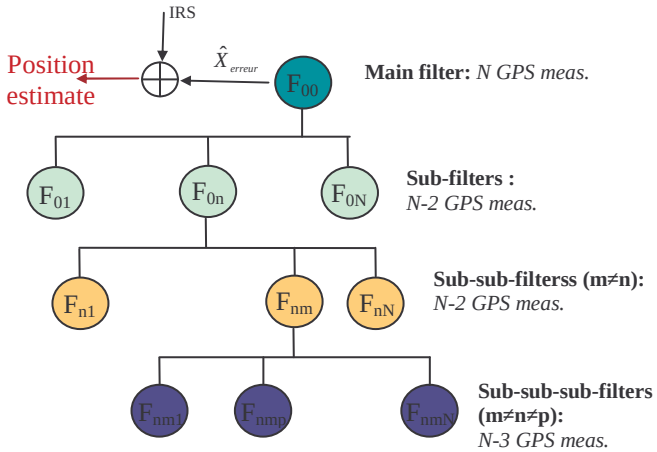

Figure 8. New Kalman filters hierarchy

Test data definition

Let $\Delta\hat{\mathbf{x}}_{mnp}$ be the state vector of sub-sub-sub-filter F_{mnp}, separation between F_{mn} and F_{mnp} is given by

$$\begin{aligned}\mathbf{dx}_{\mathbf{m}np}{}^{+}(k) &= \Delta\hat{\mathbf{x}}_{mn}{}^{+}(k) - \Delta\hat{\mathbf{x}}_{\mathbf{m}np}{}^{+}(k) \\ &= \delta\mathbf{x}_{mn}{}^{+}(k) - \delta\mathbf{x}_{\mathbf{m}np}{}^{+}(k), \\ p &= 1\ldots N, m \neq n, p \neq m, p \neq n\end{aligned} \tag{19}$$

whose statistics are described by the covariance matrix $\mathbf{dP}_{\mathbf{m}np}{}^{+}(k)$.

For each sub-sub-sub-filter the decision threshold is set so that (assuming that each filter F_{mnp} has the same chance for a false alarm)

$$D_{mnp} = \sqrt{\lambda^{dP_{mnp}}} \cdot Q^{-1}\left(\frac{P_{FD}}{2(N-2)}\right) \tag{20}$$

The next paragraph discuss with the use of P_{FD}.

The test statistic associated to D_{mnp} is

$$d_{mnp} = \left|X_{p\perp}(1)\right| \text{ or } \left|X_{p\perp}(2)\right| \tag{21}$$

Satellites r and s are excluded as the failed satellites if and only if [test3]

$d_{rsm} < D_{rsm}$ for all $m \neq r, m \neq s$

and $\forall i \neq r, \forall j \neq s, \exists k / d_{i,j,k} \geq D_{i,j,k}$

and

$d_{srm} < D_{srm}$ for all $m \neq r, m \neq s$

and $\forall i \neq s, \forall j \neq r, \exists k / d_{i,j,k} \geq D_{i,j,k}$

VI. FAILURES DETECTION AND EXCLUSION WITH A TWO-FAILURE ASSUMPTION FDE ALGORITHM

Process principle

As for one-failure FDE algorithm, the new algorithm discussed bellow is based on hypothesis testing

H_0	Normal case: no range fault
H_1	Abnormal case: one range failure
$H_n, n>1$	Abnormal case: more than one range failure

The following process is based on the experimental assumption that when there are two simultaneous range failures; filter solution which is using the two faulty measurements is far more affected by the failures than filter solution which is using only one faulty measurement. Thus the impact of the second failure is such that the test metric between a one-failure filter and a two-failure filter is always exceeding the threshold (in the same manner that, the test metric between a one-failure filter and a zero-failure filter is always exceeding the threshold).

(i) Failures detection

Detection occurs at the first row, but there is no decision taken whether there are one or two range failures. The hypothesis test is

H_0 no detection: $d_{0n} < D_{0n}$

$H_1,\ H_n, n>1$ detection: $\exists n \in \{1, N\}, d_{0n} \geq D_{0n}$

For the following points the assumption that detection occurs is made.

(ii) One-failure H_1 identification and exclusion

The identification of H_1 assumption and exclusion of the faulty satellite occurs at row 2. It is performed with the test described in section 3 of one-failure exclusion.

Satellite r is excluded as the faulty satellite if and only if

$d_{rm} < D_{rm}$ for all $m \neq r$

and

$d_{nr} \geq D_{nr}$ for all $r \neq n$

[see figure 4]

(iii) More than one failure H_n identification

The identification of H_n assumption also occurs at row 2

$H_n, n>1 \quad \forall n, \exists r \neq n / d_{nr} \geq D_{nr}$

In the two-failure assumption, this test is used as identification of H_2.

(vi) Two failures exclusion

The exclusion of the two faulty satellites occurs at row 3 according [test3].

Figure 9 is illustrating what we theoretically expect when there are two failures (points *(iii)* and *(iv)*).
Let assume that SAT1 and SAT2 are at channels 2 and 4.

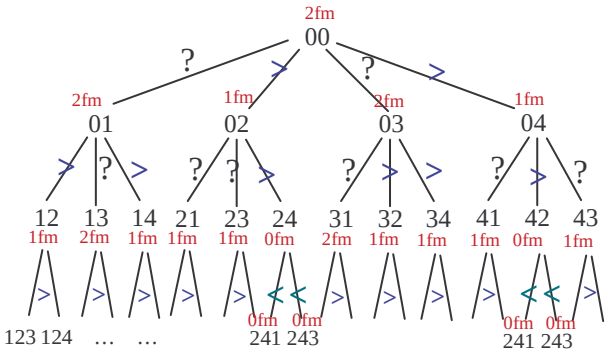

0fm Kalman filter using no faulty measurement
1fm Kalman filter using one faulty measurement
2fm Kalman filter using two faulty measurements

Figure 9. Two failures theoretical impact on tests metric.

Discussion on the use of the FDE requirements

Setting the thresholds

One-failure exclusion function

In [2], the author defines exclusion threshold as a function of P_{FD} [see equation 14] since the detection function has to be available after exclusion.
Indeed, after exclusion, the main filter and the sub-filters are re-initialized with the safety sub-filter and sub-sub-filters respectively. These last sub-sub-filters are then dedicated to detection of a next failure.

Two-failure exclusion function

The same idea has been applied to set the thresholds for the tests at the third layer of Kalman filters [see equation 20]. After exclusion of the two faulty satellites, the main filter and the sub-filters are re-initialized with the safety sub-sub-filter and sub-sub-sub-filters respectively.

Definitions of *HPL*

The *HPL* may be defined as a function of the *Integrity Risk* requirement (P_{MI})

$$\mathrm{P}[HE > HPL\ no\ alert] < P_{MI}$$

where *HE* is the horizontal error; and "*no alert*" means "without an alert during time to alert".
(for phases of flight from en-route to *NPA*, $P_{MI} = 10^{-7}/hr$ and the time to alert is $10s$).
Using H_0, H_1, H_2, the former expression may be written

$$\mathrm{P}\left\{\begin{array}{l}(HE > HPL\ no\ alert \cap H_0)\\ OR\,(HE > HPL\ no\ alert \cap H_1)\\ OR\,(HE > HPL\ no\ alert \cap H_2)\end{array}\right\} < P_{MI}$$

which is similar to

$$\begin{aligned}&\mathrm{P}(HE > HPL\ no\ alert|H_0)\cdot\mathrm{P}(H_0)\\ &+\mathrm{P}(HE > HPL\ no\ alert|H_1)\cdot\mathrm{P}(H_1)\\ &+\mathrm{P}(HE > HPL\ no\ alert|H_2)\cdot\mathrm{P}(H_2) < P_{MI}\end{aligned}$$

As for the one-failure assumption the following allocation is made

i. $\mathrm{P}(HE > HPL\ no\ alert|H_0)$ is the rare normal performance rate
ii. $\mathrm{P}(H_1)$ is the probability of having one GPS satellite failure per hour per aircraft
iii. $\mathrm{P}(HE > HPL\ no\ alert|H_1)$ is the missed detection probability in the case when there is only one satellite failure
iv. $\mathrm{P}(H_2)$ is the probability of having two GPS range failures per hour per aircraft

v. $P(HE > HPL\ no\ alert | H_{21})$ is the missed detection probability in the case when there are two range failures

The difficulty is that we need to allocate values to these probabilities.
The acknowledgment of these may allow us to give a definition of the global HPL, which would determined by the following ways

1. we calculate HPL_0 value from (i)
2. we calculate HPL_1 value from (iii)
3. we calculate HPL_2 value from (v)

with

HPL_0 Is the value of HPL for which in the fault free case,
$P(HE > HPL_0) = P(HE > HPL\ no\ alert | H_0)$

HPL_1 Is the value of HPL for which in the one range failure case,
$P(HE > HPL_1) = P(HE > HPL\ no\ alert | H_1)$

HPL_2 Is the value of HPL for which in the two range failures case,
$P(HE > HPL_2) = P(HE > HPL\ no\ alert | H_2)$

Since the global HPL has to satisfy these three conditions, in a first approach it would be defined as

$$HPL = \max(HPL_0, HPL_1, HPL_2)$$

HPL_0, HPL_1, HPL_2 can be analytically calculated using $\mathbf{P}_{00}^{+}[7:8,7:8]$, $\mathbf{P}_{0n}^{+}[7:8,7:8]$ and $\mathbf{P}_{nm}^{+}[7:8,7:8]$ [see section 3].

At the current time, no value is calculated for HPL_2 as $P(H_2)$ is not allocated and requires further discussion.

Definitions of HEL

In the one-failure assumption, by adding "the requirement that detection must be possible after exclusion has occurred […] HEL is given by the largest HPL of the subsets of $(N-1)$ satellites" [9] [see Chapter 3]. Let us denote it HEL_1.

In the case of multiple-failure assumption we could also calculate HEL_2.
HEL_2 would be given by the largest HPL of the subsets of $(N-2)$ satellites under the condition that detection must be possible after exclusion has occurred.
And HEL would be the maximum of HEL_1, HEL_2.

The definition of HEL_2 and so forth HEL is only assumption, and requires further analysis.

Simulation results

With similar assumptions than those taken at chapter IV, we get the following result with the process presented above

- Table 7: simulation hypothesis
- Figure 10 and Table 8: simulation results on position error

The process succeeds in isolating the two faulty satellites and after isolation the main Kalman filter is re-initialized with F_{39}.

Number of tracked satellites = 9, t_0 = 300s		
SAT1	channel: 3	error size: 0.7m/s
SAT2	channel: 9	error size: 1m/s

Table 7: Simulation hypothesis

Delay after t_0	
Failures detection	60s
Identification of H_2	70s
Exclusion	118s

Table 8: Times of detection and isolation

We can notice that the identification of the presence of two failures occurs soon after the algorithm is detecting failures.

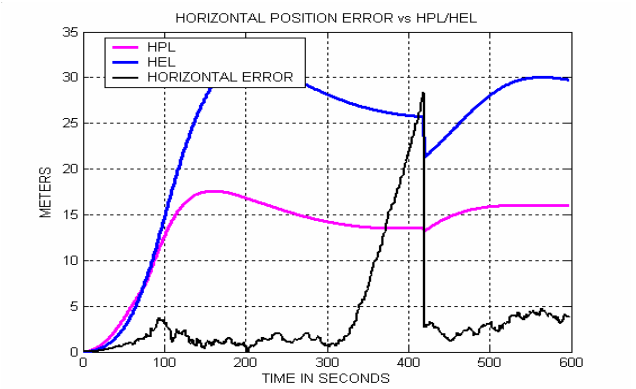

Figure 10: Horizontal position error vs HPL/HEL

HPL and HEL which are presented on this figure are HPL computed at the first row of filters hierarchy and HEL calculated at the second row. They are standing for the one-failure FDE algorithm levels and are not representative of the whole process. As mentioned in chapter VI, we have not clearly defined a global HPL / HEL, which could be compared to HAL in order to appreciate the availability of the process.
Yet the horizontal error at the output of the system is very bellow the HAL defined for the non-precision approach phase of flight (556m), and thus it can't involve an alert.

VII. SUMMARY AND CONCLUSION

Despite the fact that the occurrence of multiple simultaneous range failures is a roughly unlikely event when failures are independent, it can become more important in the case of jamming.

This paper presents a hypothesis test which is being investigated at the ENAC in order to use the GPS/IRS hybridization Solution Separation integrity monitoring method under the assumption that two simultaneous range failures can occur. The paper also proposes the integration of this test with the current one-failure FDE algorithm to form three test levels.

Practically, the detection of failures occurs at the first level.

In case of one failure, the exclusion of the faulty satellite - as well the identification of the one-failure hypothesis – is performed at the second level.

In case of two failures, due to the fact that the FDE process is based on hypothesis testing, the simulations which were conducted have shown that the failures may have simultaneous or delayed impact on the test metrics. In the first case, the tests allow identifying the two-failure hypothesis at the second level, and the two faulty measurements are excluded with the tests at the third level. In the second case, the tests at the second level allow identifying two successive failures and excluding them.

Thus the FDE function can be performed either by a one-failure assumption or by a two-failure assumption algorithm.

The definitions of global *HPL* and *HEL* are not clearly laid down and doesn't allow us to completely appreciate the performance of the process.

REFERENCES

1. M. BRENNER, Integrated GPS/inertial detection availability, Journal of The Institute of Navigation, Sept. 1995.
2. K. VANDERWERF, FDE Using Multiple Integrated GPS/Inertial Kalman Filters in the Presence of Temporally and Spatially Correlated Ionospheric Errors, ION GPS 2001, 11-14 Sept. 2001, Salt Lake City
3. Requirements and Test Procedures for Tightly Integrated GPS/Inertial Systems Appendix R to DO-229C
4. J. C. RADIX, Systèmes Inertiels à Composants Liés "Strapdown", Cépadues Educs, 1991
5. R. DA, Investigation of a Low-Cost and High-Accuracy GPS/IMU System, Proceedings of ION GPS, Sept. 1996
6. FARRELL J. A., BARTH M., The Global Positioning System & Inertial navigation, McGrow-Hill, 1998
7. BROWN R. G., Solution of the Two-Failure GPS RAIM Problem Under Worst-Case Bias Conditions: Parity Space Approach, navigation Journal of the Institute of Navigation, Vol. 44, No. 4, Winter 1997-1998
8. RTCA/DO-229, Minimum operational performance standards for global positioning system / wide area augmentation system airborne equipment RTCA SC-159, January 16, 1996
9 LEE Y., VAN DYKE K., DECLEENE B., STUDENNY J., BECKMAN M., Summary of RTCA SC-159 GPS Integrity Working Group Activities, Global Positioning System – Papers published Navigation – Redbook Volume V, 1998, p195-226